

# Development and Testing of a New Type of MPD Thruster<sup>#\*</sup>

V.B. Tikhonov\*, N.N. Antropov\*, G.A. Dyakonov\*, V.A. Obukhov\*,  
F. Paganucci\*\*, P. Rossetti\*\*, M. Andrenucci\*\*.

\* RIAME MAI, 125080 Moscow, PB 43, Russia

\*\*CENTROSPAZIO, Via Gherardesca, 5, 56014, Pisa, Italy

IEPC-01-123

Numerous experiments on magneto-plasma-dynamic thrusters (MPDT) have shown that the limitation of propellant exhaust velocity and thrust efficiency is due to an ion-sound instability occurring at the near-anode zone of the discharge. It was suggested an injection of pre-ionized propellant throughout the anode to increase the ion density in the near-anode zone and thus alleviate the onset of plasma instability. To assess the effectiveness of this solution, a new MPDT (called "Hybrid Plasma Thruster - HPT) has been developed. The HPT consists of two stages (chambers) divided by a half-transparent anode. The first stage serves for the preliminary ionization of part of the propellant (10-15%) and the second one is used for ionization and acceleration of the total plasma flow (up to 10-15 km/sec). Two HPT prototypes with an external magnetic field has been developed and independently tested in RIAME and Centrosazio, using nitrogen and argon as propellants. The paper describes the thruster, the experimental apparatus and the main results obtained so far, in terms of electrical characteristic and thrust. Tests have shown the activation of the additional discharge in the ionization chamber leads to the substantial decrease of both the discharge voltage and the ion-sound oscillations with typical frequency of about 100 kHz., confirming the HPT concept is worth being further investigated.

## Introduction

The most attractive features of Magneto-Plasma-Dynamic Thrusters (MPDT's) for space applications are the high thrust density (up to  $10^4 N/m^2$ ), the design simplicity, the robustness and the possibility, in principle, to use a large variety of propellants (gases, polymers, alkali metals). These features allow the MPDT's to be favorably considered for high power (0.1-1 MW), primary missions, ranging from orbit-raising of large satellites to cargo interplanetary transfer. For this last class of missions, MPDT's represent almost the unique electric propulsion option,

provided an exhaust velocity of 40-60 km/s, a thrust efficiency larger than 50% and a lifetime of 5-10 thousands hours are exhibited [1]. However, the achievement of these performance is generally hampered by the occurrence of detrimental phenomena, usually referred as "onset phenomena", taking place when a critical current is exceeded, depending on thruster geometry, propellant and mass flow rate. Onset phenomena involve arc voltage fluctuations, power losses and, eventually, strong erosion or melting of thruster components (anode in particular). Several experiments show the critical current is close to the full ionization current, at which all the propellant is ionized and exhausted at the

<sup>#</sup> Presented as Paper IEPC-01-123 at the 27<sup>th</sup> International Electric Propulsion Conference, Pasadena, CA, 15-19 October, 2001.

\* Copyright © 2001 Centrosazio, Riame. Published by the Electric Propulsion Society with permission.

critical Alfvén velocity and the near-anode zone is the most involved region in onset phenomena [2, 3]. This last occurrence is attributed to the joint action of pinch and Hall effect, which tends to compress the plasma to the thruster axis and, consequently, to reduce plasma density in the anode region. The relevant increase of the Hall parameter in the anode layer yields an increase of the anode potential drop and electron temperature. This occurrence is favorable for the development of ion-sound microinstability, which, in turns, increases plasma thermalization and heat transferred to the anode. Direct injection of neutral propellant in the anode region has proved to alleviate and/or delay the onset phenomena [4]; nevertheless no decisive results have been obtained, since the ionization length in MPDT's exceeds the anode layer extent (of the order of the electron Larmor radius): an injection of ionized propellant in the anode region seems thus more appropriate to modify the anode layer condition, as shown in [5]. To assess the effectiveness of this last solution, a new MPDT (called "Hybrid Plasma Thruster" - HPT) has been proposed [6], developed and tested in the framework of a joint activity between RIAME of the Moscow Aviation Institute (RU) and Centrospazio (Pisa, I). On the basis of the results of a performance model [7], two almost identical prototypes have been developed and are currently under testing in each laboratory. Some of the experimental results gathered so far are illustrated in the following.

### The Hybrid Plasma Thruster

The HPT is an axisymmetric MPD thruster with an applied magnetic field, a central acceleration chamber and a peripheral ionization chamber. Each prototype developed consists of:

- a central hollow cathode (copper, 20 mm in dia);
- an anode, consisting of a cylinder (aluminum, 200 mm in inner dia for the CS prototype; stainless steel, 190 mm in the inner dia for the RIAME prototype) and eight straps, made of copper, which divide the central chamber from the ionization chamber. To optimize the acceleration processes in the central chamber, the straps are shaped to be parallel to the local magnetic force lines;
- eight peripheral hollow cathodes (copper, 12 mm in dia each);
- a solenoid, capable of producing an induction field up to 100 mT at the thruster axis.

Since the prototypes operate in a pulsed, quasi-steady mode, the insulators between the electrodes are currently made of Plexiglas™.

Fig. 1 shows the HPT prototype available at Centrospazio.

The aim of the peripheral chamber is the ionization of a small fraction of the propellant by means of a secondary, low power discharge between the peripheral cathodes and the anode. The ionized propellant then flows in the acceleration chamber, increasing plasma density near the anode. A relevant onset phenomena reduction is expected. In [7] an anode voltage drop reduction up to 10 V at the critical condition is estimated, due to the added ionized gas.

The acceleration processes taking place in the HPT are mainly electromagnetic. In the region close to the central cathode, the thrust is mainly generated by the interaction between the radial current and the self-induced, azimuthal induction field. In the anode region of the acceleration chamber, where the electron Hall parameter should be moderately higher than 1, the main contribution to thrust comes from the interaction between the azimuthal Hall current and the applied magnetic field, similarly to an SPT operation. [7] indicates the Hall effect contribution to thrust is always significant up to the critical current and can represent the main contribution, especially at low mass flow rates and currents.

Main differences between the two prototypes concern the electric power supply system and the gas feeding system as well.

The HPT prototype at the RIAME laboratory is provided with two separate circuits for the power supply of the discharge in the accelerating chamber (Forming Line 1, FL1) and of the discharge in the ionization chamber (FL2), as illustrated in Fig. 2. Discharge is initiated by an IRT-6 ignitron, on the FL1 circuit, while the FL2 circuit is free from switches and is switched on independently at the discharge evolution in the accelerating chamber. Maximum charging voltage of capacitors is  $U_o = 1600$  V to provide a stored energy up to 1536 J in both power supply lines. Duration of the current pulse in both chambers has been set to 700 ns. The currents signals of the primary discharge  $J$  and of the discharge in the ionization chamber  $J_a$ , recorded at  $U_o = 1000$  V are shown in Fig. 3. An electromagnetic, disk-type gas valve provides gas impulses about 1 ms long; the gas, typically argon or nitrogen is injected through the central cathode at a flow rate from  $10^{-6}$  to  $10^{-5}$  Kg per impulse. With respect to the valve opening, the

electrical discharge is switched on with a delay of  $0.5\text{ ms}$ ; in this condition the total operating volume of the thruster, comprising the ionization chamber, is filled by propellant before electrical discharges occur. This method of anode gas feeding was successfully used in the quasi-stationary accelerators of QSPA type [8]. The main disadvantage of this type of gas feeding is the impossibility to control gas consumption in both chambers as in the prototype of CS. The magnetic coil is supplied with the direct current  $J_m \sim 15\text{ A}$ , at which calculations showed to correspond a magnetic field induction of  $0.03 - 0.04\text{ T}$  in the thruster accelerating channel.

For the HPT prototype developed at CS, the electric power is supplied by a Pulse Forming Network (PFN), connected as shown in Fig. 4, capable of deliver quasi-steady current pulse  $1-5\text{ ms}$  long with instantaneous power of  $100-800\text{ kW}$  in the primary circuit and of  $5-40\text{ kW}$  in the secondary one. The propellant is injected by two gas feeding systems, one for the central cathode and the other for the peripheral cathodes, based on fast acting solenoid valves, which provide gas pulses with long plateau after few milliseconds from valve activation [2]. When a steady state mass flow is reached, the electric circuit is closed by switching an ignitron on and the discharge takes place. The solenoid is supplied by a DC generator, switched on few seconds before the discharge. Figs. 5 and 6 show typical current and voltage signals respectively for a pulse length of about  $2.5\text{ ms}$ .

### Preliminary Experimental Results at RIAME

The HPT prototype at the RIAME lab has operated with nitrogen as propellant. The thruster is mounted on a  $1\text{-m}^3$  vacuum chamber maintained to a pressure of  $10^{-4}\text{ torr}$  during shots.

Signals of current  $J(t)$  and voltage  $U(t)$  referring to the acceleration chamber at two different FL1 charge voltages  $U_o$  are reported in Figs. 7 and 8. For both conditions the gas flow rate is  $2\text{ g/s}$  and the FL2 charge voltage  $U_{oa}$  is  $1000\text{ V}$ , corresponding to an electric power of about  $50\text{ kW}$ .  $U_1(t)$  signal has been obtained without applying the external magnetic field (the self magnetic field acceleration (SMFA) mode) and without the discharge in the ionization chamber;  $U_2(t)$ ,  $U_3(t)$  signals correspond to the external magnetic field acceleration (EMFA) mode, without and with the ionization chamber activation respectively.

All the voltage signals appear free from significant oscillations up to  $t = 300 - 400\text{ ns}$ , afterwards oscillations typical of the crisis regime can be observed. This phenomenon is probably related to the modality of gas injection through the central cathode with respect to the electric pulse: after the time  $t$ , the anode region, filled by propellant in the pre-discharge phase, begins to be poor of gas particles.

With the activation of the discharge in the ionization chamber the amplitude of those oscillations somewhat decreases.

Electrical characteristics for the thruster operating in the SMFA mode (1) and in the EMFA mode (2) are given in Fig. 9. To exclude the inductive component of the discharge voltage ( $U_i = LdJ/dt$ ), the current and voltage values at the maximum in the  $J(t)$  signal have been considered. Bars on data points show the amplitude of voltage signal oscillations. Volt-ampere characteristics are linear, which is usual for sub-crisis regimes of plasma acceleration.

In a successive experiment, in order to approach the crisis regime, the gas valve was adjusted for a lower flow rate:  $0.2\text{ g/s}$ . Initial voltage of FL1 capacitor bank has been  $U_o = 800; 1000; 1200; 1400$  and  $1600\text{ V}$ . For each  $U_o$  value, current and voltage signals have been taken with thruster operating in the following four modes: (1) SMFA mode and without the discharge in the ionization chamber; (2) SMFA mode and with the discharge in the ionization chamber; (3) EMFA mode and without the discharge in the ionization chamber, (4) EMFA mode and with the discharge in the ionization chamber. The FL2 capacitor bank has been always charged to  $U_{oa} = 1000\text{ V}$ .

Figs.10 – 12 report for three different value of  $U_o$ , the corresponding current signal  $J(t)$  and voltage signals  $U_1(t)$  and  $U_2(t)$ , referring to thruster operation without and with the ionization chamber activation respectively. The voltage signals are modulated by oscillations with a characteristic frequency  $f \sim 100\text{ kHz}$ , meaning the thruster has operated in the close-to-crisis regime.

The electrical characteristics of the thruster operating in the SMFA mode and in the EMFA mode are shown in Fig. 13 and 14; again the current and voltage values considered correspond to the maximum in the current signal and the bars extension reflects the amplitude of voltage signal oscillations. Results seem demonstrate the benefic effect of the peripheral chamber on thruster operation for all the conditions examined: with the ionization chamber activation the voltage is lower and

besides the amplitude of the oscillations of the voltage signal somewhat decreases.

It is not usual for the crisis mode operation that the volt-ampere characteristics are practically linear up to the value of the discharge current  $J \sim 3.5 \text{ kA}$ , well above the estimated critical current. Abrupt growth of the discharge voltage for both SMFA and EMFA modes has been not observed. Probably, at high values of current the erosion of the central cathode rises sharply and the mass consumption grows. As a result the discharge voltage decreases. Theoretical considerations show that the depleted material rate from the copper cathode operating in the spot emission regime is of the order of  $0.1 \text{ g/s}$ , a value comparable to the nitrogen flow rate; moreover the ionization potential for copper is  $U_{icu} = 7.7 \text{ eV}$ , much lower than for nitrogen ( $U_{in} = 14.5 \text{ eV}$ ). So copper atoms ionization in the near-cathode region can appreciably decrease the thruster voltage or increase the discharge current. In the future the use of tungsten cathodes is necessary. It can be expected that with tungsten cathodes the erosion effect on the  $V$ - $I$  curve will be reduced since tungsten has a lower mass transfer coefficient ( $K_m \sim 10^{-8} \text{ kg/C}$ ) than copper ( $K_m \sim 10^{-7} \text{ kg/C}$ ).

### Preliminary Experimental Results at CS

Electrical characteristic and thrust measurements performed at Centropazio with argon as propellant are shown below. The thruster is mounted on a thrust stand inside a vacuum chamber, capable of maintaining a back pressure within  $10^{-4} \text{ mbar}$  range. Thrust ( $T$ ) measurements have been carried out with a ballistic method [2], which allows instantaneous thrust to be obtained with an overall accuracy within  $\pm 10\%$  of the data points. Each data point of the electrical characteristics has been obtained as an average of current and voltage on a window  $100$  microseconds long taken in the middle of the pulse. Current values reported on the  $x$ -axis refer to the primary circuit, while each voltage value has been calculated as:

$$V = V_1 + (I_2 / I) V_2$$

where subscripts 1 and 2 refer to the acceleration and ionization chamber respectively. In this way, the  $VxI$  product represent the total power consumed by the thruster (except for the solenoid circuit). The overall voltage and current accuracy is within  $\pm 4\%$  and  $\pm 3\%$  of the data points respectively.

Figs. 15 and 16 show the electrical characteristics measured for  $660 \text{ mg/s}$  of argon and an applied magnetic field with a maximum induction on the axis of  $40 \text{ mT}$  (calculated). Three cases have been investigated: all the propellant injected from the central cathode without activation of the ionization chamber,  $600 \text{ mg/s}$  from the central cathode and  $60 \text{ mg/s}$  from the peripheral cathodes with and without activation of the ionization chamber. A reduction of the primary arc voltage (about  $5 \text{ V}$ ) with the activation of the ionization chamber was observed for  $660 \text{ mg/s}$  below the estimated critical current. No significant reduction was observed for higher currents.

Fig. 17 shows the thrust data obtained at  $660 \text{ mg/s}$  with and without the external magnetic field. The HPT operation without applied magnetic field seems to be well represented by the model  $T = bI^2$  for  $I < I_{ci}$  and  $T = bI_{ci}I$  for  $I \geq I_{ci}$  ( $b = 1.8 \times 10^{-7} \text{ N/A}^2$ ) [2], where  $I_{ci}$ , the critical ionization current, is about  $5600 \text{ A}$ . The applied magnetic field seems to improve the thrust up to a current level not far from the full ionization current without the applied field, no matter the ionization chamber is activated, while for higher currents no significant thrust augmentation seems to occur. Since the Hall effect contribution to the thrust is mostly generated in the anode region, we believe this region is poorer and poorer of propellant by increasing the current, due to pinch effect, and consequently the Hall effect contribution to thrust decreases and is almost negligible for higher currents. A similar behavior has been observed during a more recent experimental activity on the same thruster, as illustrated in [9].

### Conclusions

Results from experimental studies carried out at CS and RIAME on two different prototypes seem to support the hybrid plasma thruster concept.

Using nitrogen as propellant, the activation of the additional discharge in the ionization chamber leads to a considerable discharge voltage decrease and to the attenuation of the ion-sound oscillations with the typical frequency of  $100 \text{ kHz}$ , both with and without the external magnetic field.

Applying an external magnetic field of about  $40 \text{ mT}$ , the critical current value decrease while the ion-sound oscillations increase. On the contrary, at higher flow rate onset phenomena are drift to higher current values.

Using 660 mg/s of argon as propellant, preliminary results gathered at CS indicate the substantial effectiveness of the ionization chamber for current up to 4000 A and of the applied magnetic field up to 5000 A, while no significant effects have been observed at higher currents.

Severe cathodes erosion due to the spotty arc attachment has been observed after operation in both prototypes.

In a whole results from the experimental investigation seem confirm the correctness of theories at the base of the HPT concept; moreover they have given precious indications for some thruster design improvements and for the future experimental activity on performance measurement.

Finally a deeper insight on HPT operation could be obtained from plasma diagnostics in the anode region; some preliminary results are already available [10].

### References

- [1] R. H. Frisbee, N. J. Hoffman, "Electric Propulsion Options for Mars Cargo Missions", AIAA paper, 32<sup>nd</sup> Joint Propulsion Conf. (JPC), Lake Buena Vista (FL), July 1996.
- [2] M. Andrenucci et al., "Scale and Geometric Effects on the Performance of MPD Thrusters", AIAA 92-3159, 28<sup>th</sup> JPC, Nashville, TN, July 1992.
- [3] M. Andrenucci, F. Paganucci, A. Turco, "MPD Thruster Plume Diagnostics", IEPC-93-141, 23<sup>rd</sup> International Electric Propulsion Conference (IEPC), Seattle, WA, Sept., 1993.
- [4] F. Paganucci, M. Andrenucci, "MPD Thruster Performance Using Pure Gases and Mixtures as Propellant", AIAA-95-2675, 31<sup>st</sup> JPC, San Diego, CA, July 1995.
- [5] N. V. Belan, V. Kim, A. I. Oransky, V. B. Tikhonov, "Stationary Plasma Thrusters", Kharkov, 1989, (in russian).
- [6] V.B. Tikhonov, G.A. Dyakonov, "MPD Thruster with External Magnetic Field and Ionization Chamber", IEPC-95-121, 24<sup>th</sup> IEPC, Moscow, 1995.
- [7] V. B. Tikhonov, V. Obukhov, G. Dyakonov, "Development and Tests of a Hybrid Plasma Thruster", Review Report no. 1, Centrospazio Contract no. 03650, 1997.
- [8] Dyakonov G.A. and Tikhonov V.B., Experimental Investigations of Influence of Accelerating Channel Geometry and External Magnetic Field on Modes of Plasma Flow in Coaxial

Quasistationary Plasma Accelerator of ? – 50 A Type, Plasma Physics, 1994, vol.20, no 6.

[9] F. Paganucci, P. Rossetti, M. Andrenucci, V.B. Tikhonov, V.A. Obukhov, "Performance of an Applied Field MPD Thruster", IEPC-01-132, 27<sup>th</sup> International Electric Propulsion Conference, October 14-19, 2001, Pasadena, CA.

[10] G. Serianni, V. Antoni, N. Vianello, P. Rossetti, F. Paganucci, M. Andrenucci, ".Plasma Diagnostics in an Applied Field MPD Thruster", IEPC-01-135, 27<sup>th</sup> International Electric Propulsion Conference, October 14-19, 2001, Pasadena, CA.

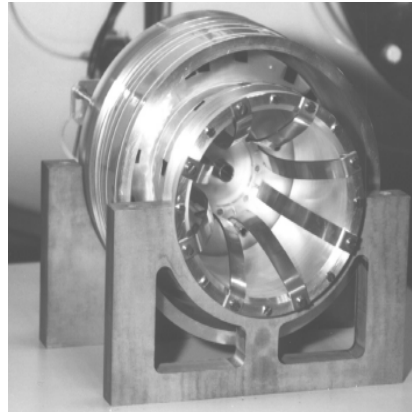
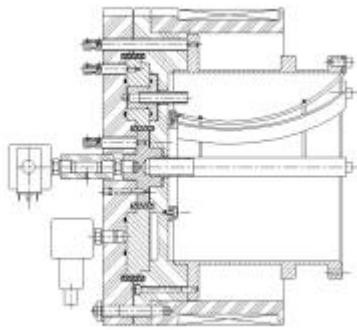


Fig. 1 – Centrosazio's HPT.

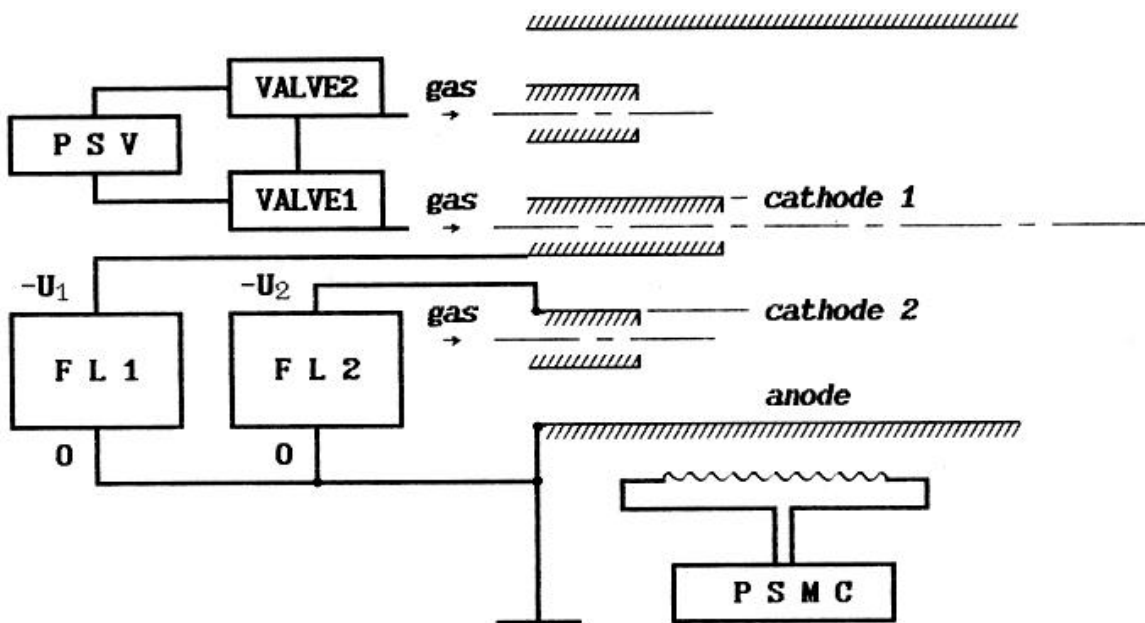


Fig. 2 – Main electric circuit arrangement (RIAME)

FL1, FL2 - forming lines;  
 PSV - power supply unit of valves;  
 PSMC - power supply unit of magnetic coil.

### Hybrid thruster currents

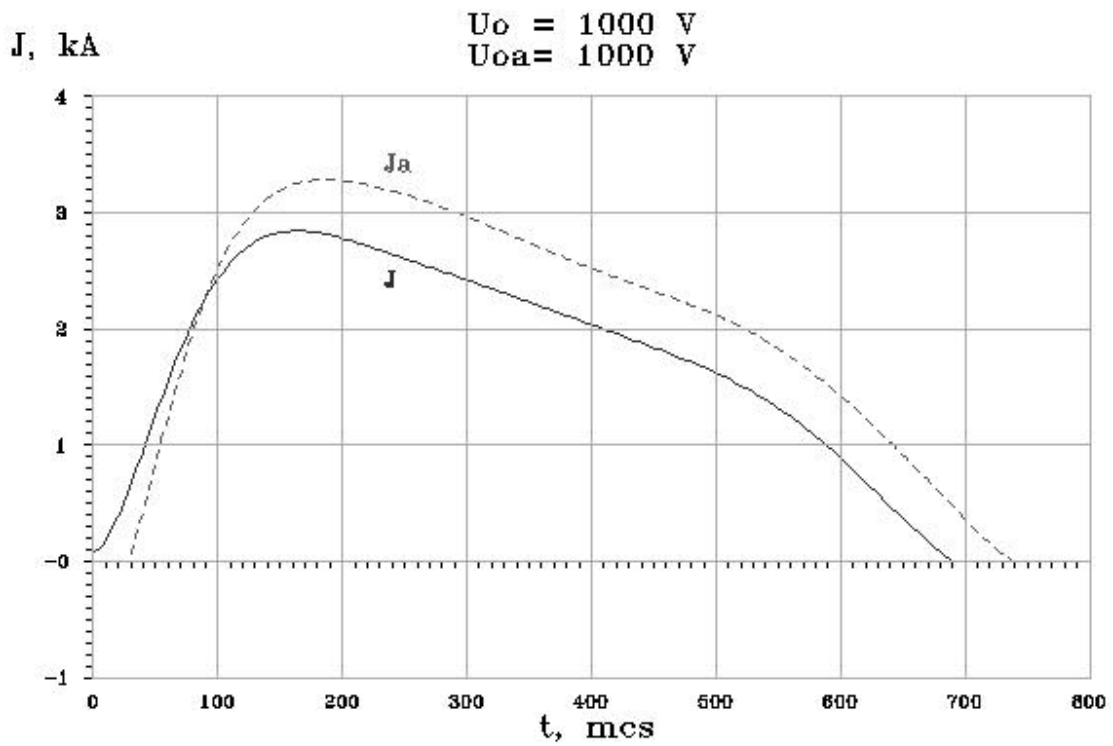


Fig.6

Fig. 3 – Current signals in the primary ( $J$ ) and secondary ( $J_a$ ) circuit.

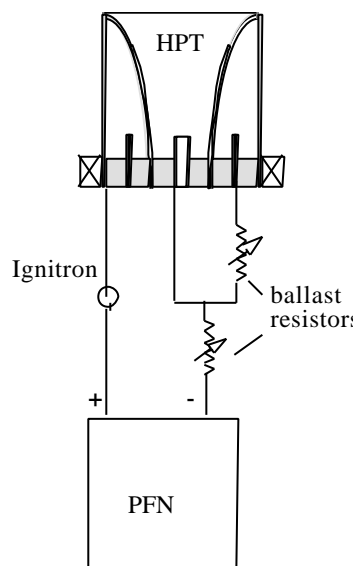


Fig.4 – Main electric circuit arrangement (Centrosazio).

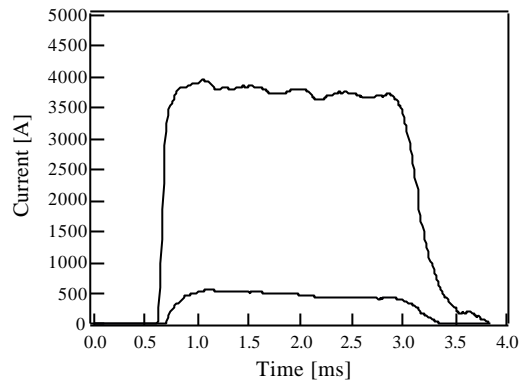


Fig.5 - Current signals (high: primary current, low: ionization chamber current) (Centrosazio).

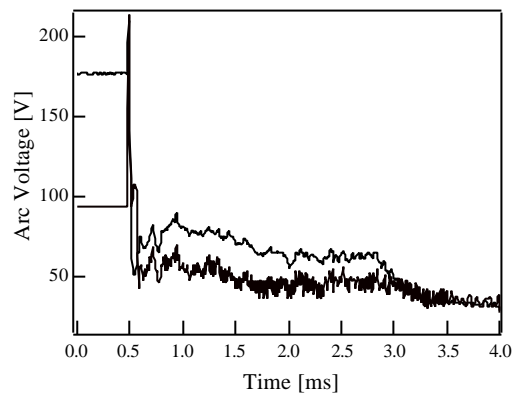


Fig. 6 – Voltage signals (high: primary voltage; low: ionization chamber voltage) (Centrosazio).

Current and voltage oscillograms

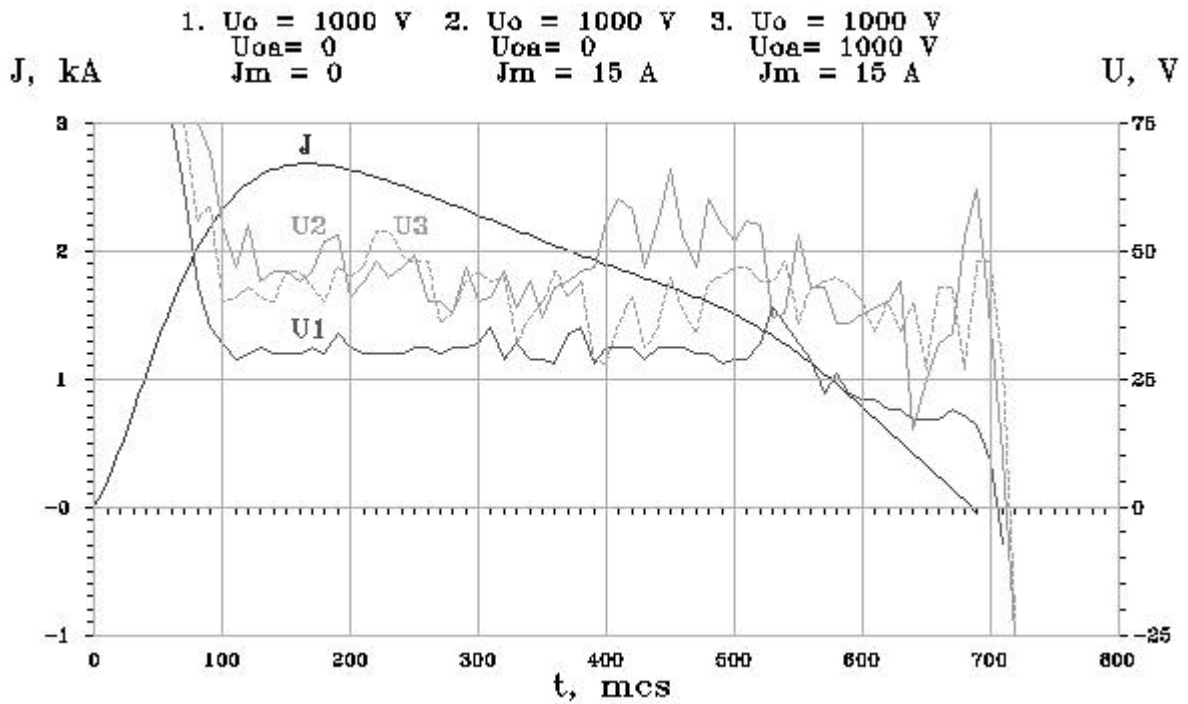


Fig.13

Fig. 7 – Voltage and current signals in the primary circuit in the sub-crisis regime at  $U_0=1000\text{V}$ .

Current and voltage oscillograms

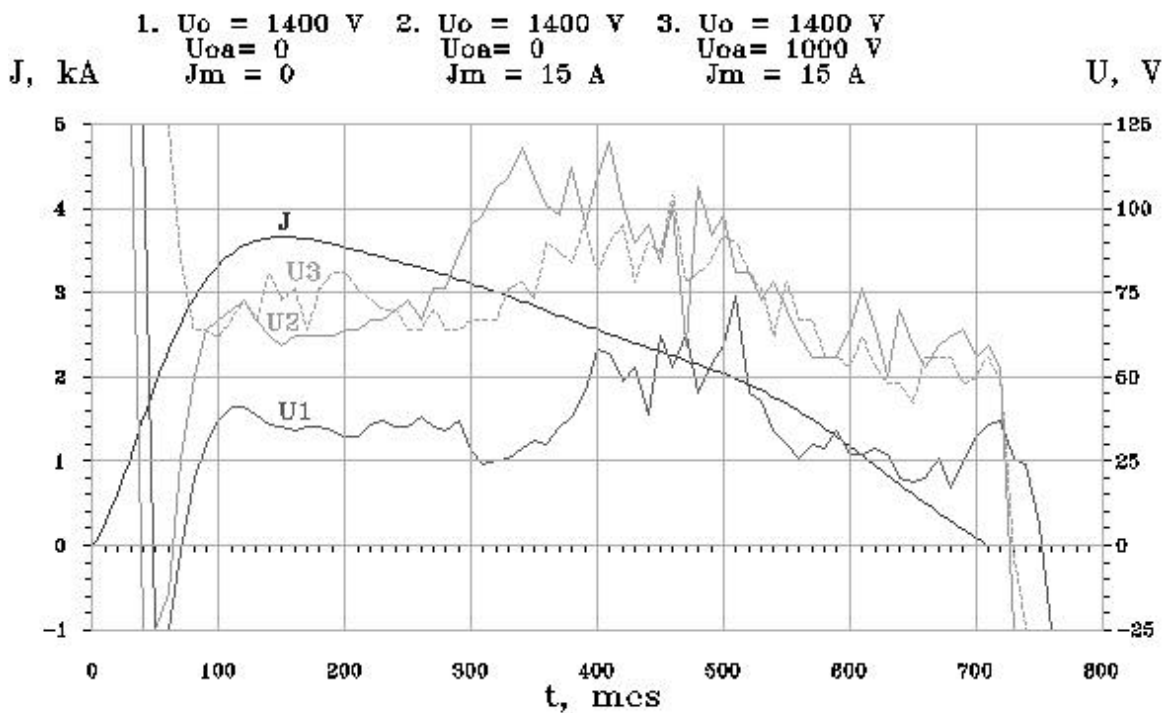


Fig.14

Fig. 8 – Voltage and current signals in the primary circuit in the sub-crisis regime at  $U_0=1400 \text{ V}$ .

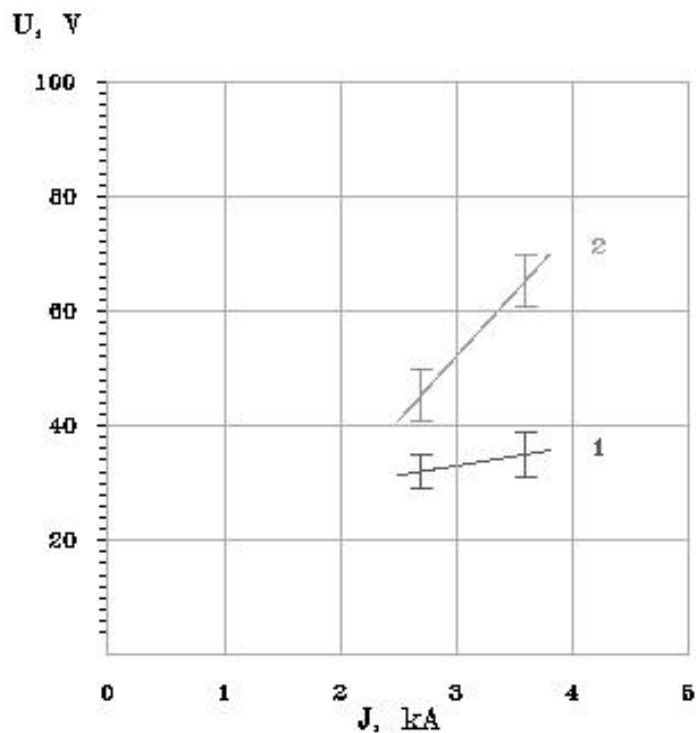


Fig.15

Fig. 9 –Electrical characteristic for the SMFA (1) and for the EMFA(2) mode.

Current and voltage oscillograms

- |                          |                           |
|--------------------------|---------------------------|
| 1. $U_0 = 800 \text{ V}$ | 2. $U_0 = 800 \text{ V}$  |
| $U_{oa} = 0$             | $U_{oa} = 1000 \text{ V}$ |
| $J_m = 0$                | $J_m = 0$                 |

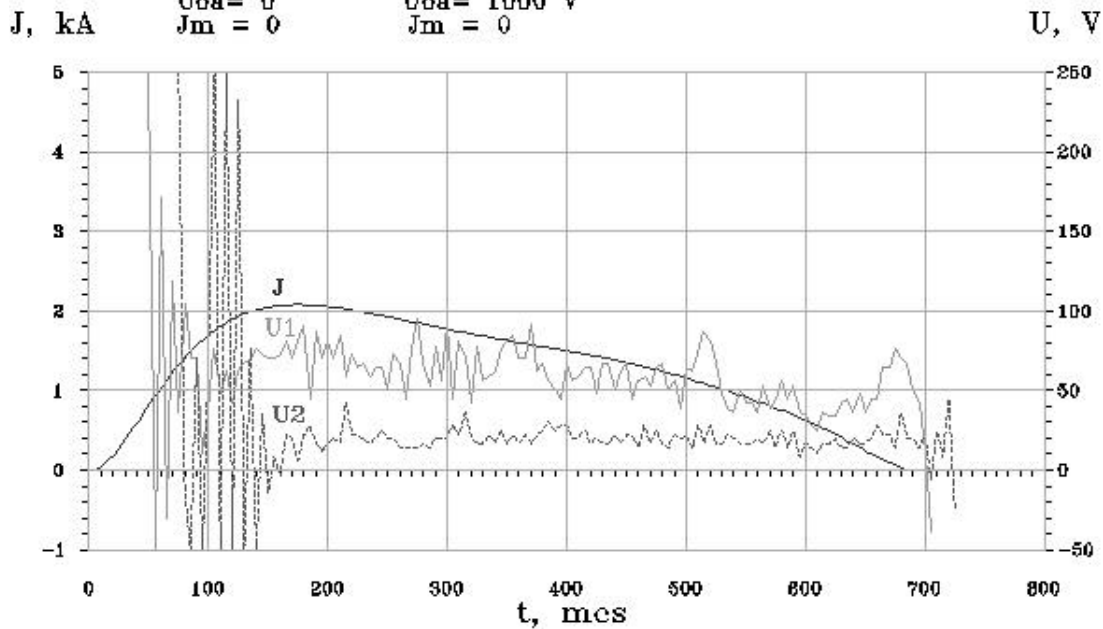


Fig.16

Current and voltage oscillograms

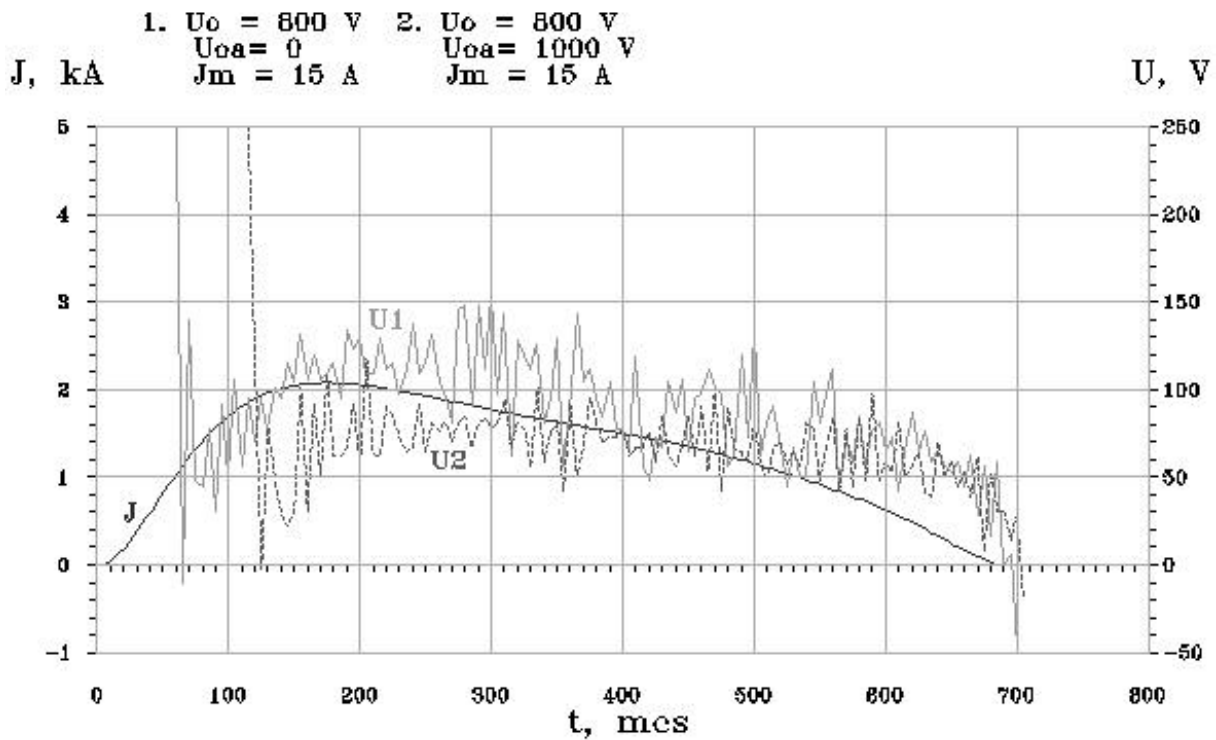


Fig.17

Fig. 10 – Voltage and current signals in the primary circuit at  $U_0=800 \text{ V}$ .

Current and voltage oscillograms

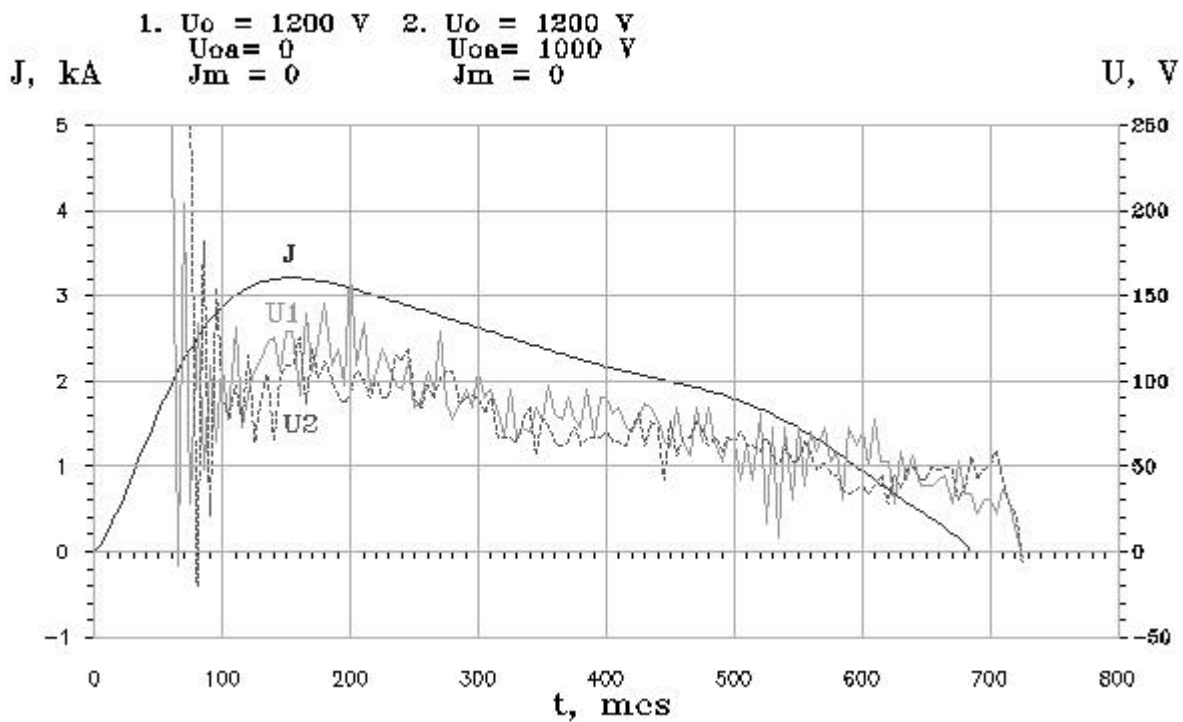


Fig.20

Current and voltage oscillograms

- |                   |                   |
|-------------------|-------------------|
| 1. $U_o = 1200$ V | 2. $U_o = 1200$ V |
| $U_{oa} = 0$      | $U_{oa} = 1000$ V |
| $J_m = 15$ A      | $J_m = 15$ A      |

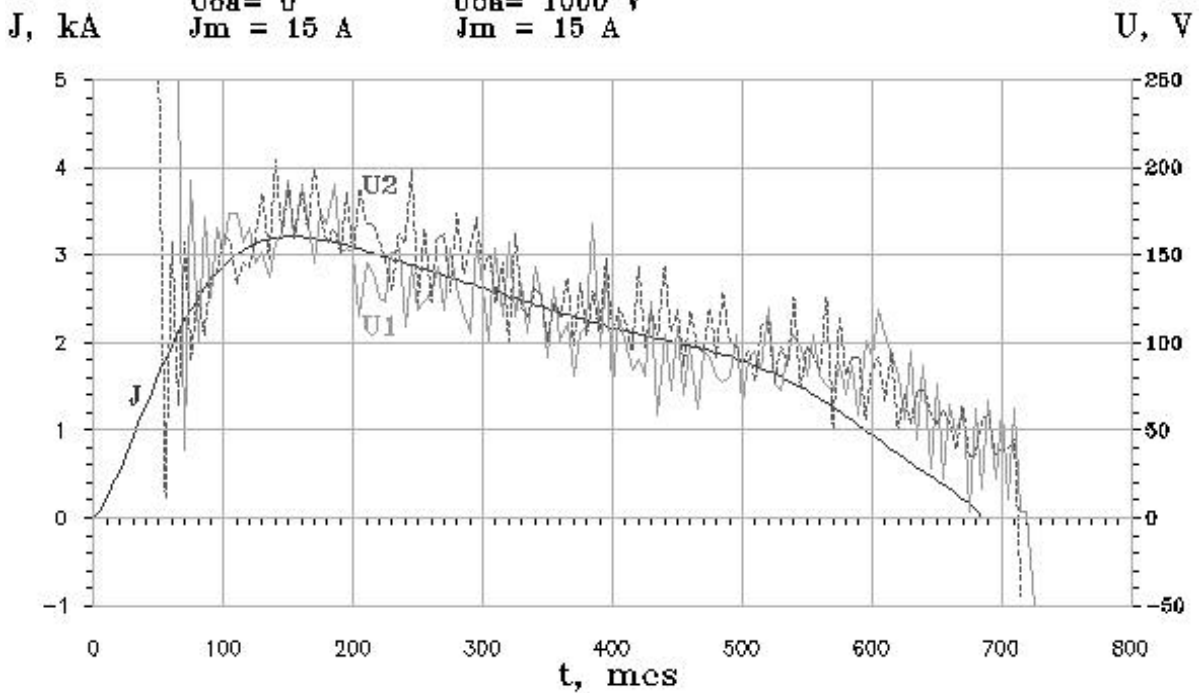


Fig.21

Fig. 11 – Voltage and current signals in the primary circuit at  $U_o=1200$  V.

Current and voltage oscillograms

- |                   |                   |
|-------------------|-------------------|
| 1. $U_o = 1600$ V | 2. $U_o = 1600$ V |
| $U_{oa} = 0$      | $U_{oa} = 1000$ V |
| $J_m = 0$         | $J_m = 0$         |

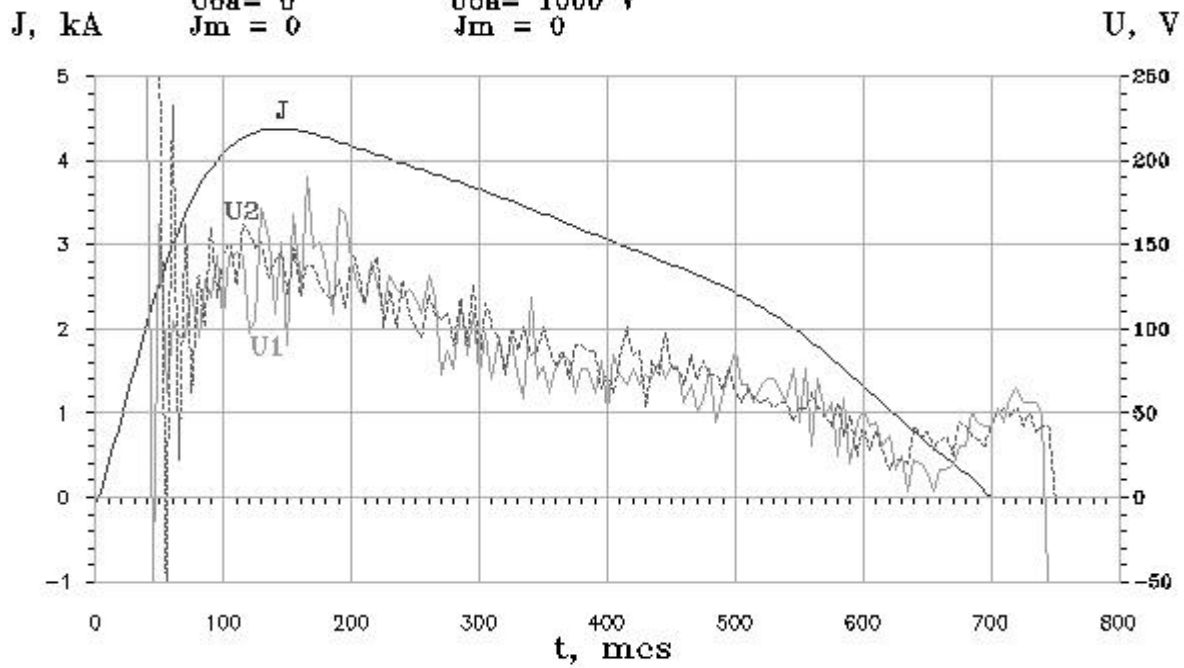


Fig.24



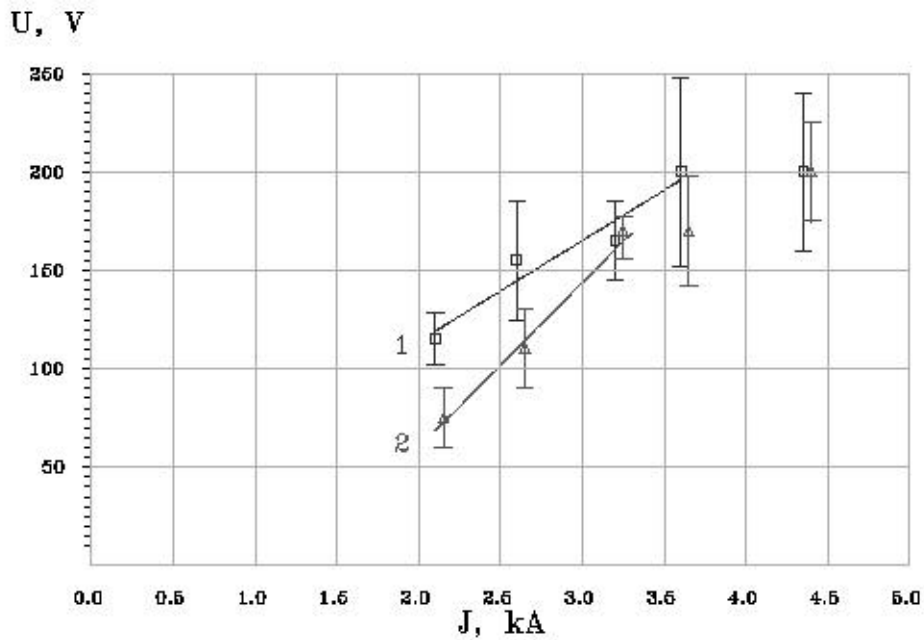


Fig-27

Fig. 14 –Electrical characteristic with (2) and without (1) the ionization chamber activation for the EMFA mode.

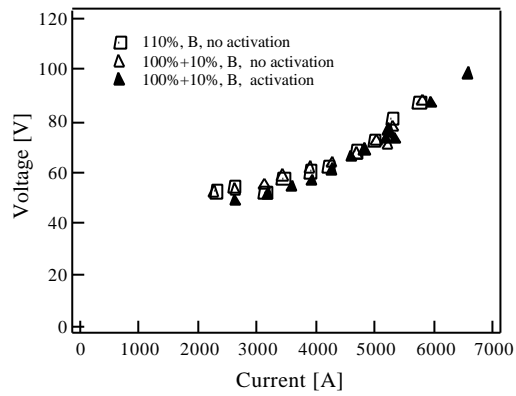


Fig. 15 – Electrical Characteristics (660 mg/s, argon).

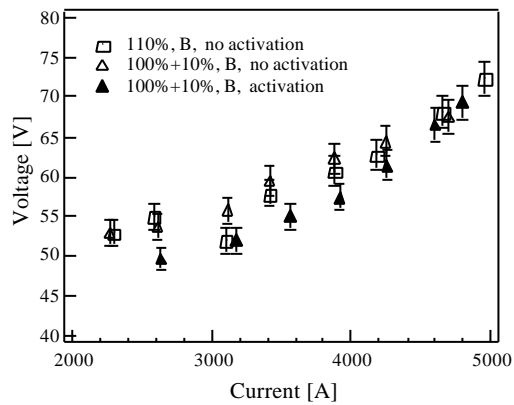


Fig.16 – Electrical Characteristics (660 mg/s, argon, zoom).

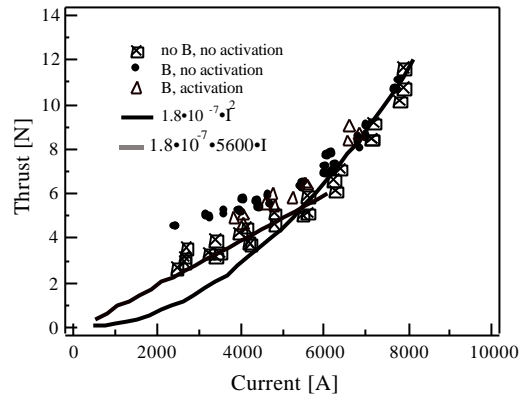


Fig. 17 – Thrust vs Current (660 mg/s, argon).